

Surface-Catalyzed Chromium(VI) Reduction: The TiO_2 - Cr^{VI} -Mandelic Acid System

BAOLIN DENG[†] AND ALAN T. STONE*

Department of Geography and Environmental Engineering,
G. W. C. Whiting School of Engineering, The Johns Hopkins
University, Baltimore, Maryland 21218

As part of a study exploring the pathways and rates of Cr^{VI} reduction under environmentally relevant conditions, this paper examines the kinetics and mechanism of Cr^{VI} reduction by mandelic acid in the presence of 1.0 g/L TiO_2 . The redox reaction is dramatically catalyzed by the oxide surface, and benzoylformic acid and benzaldehyde are the major products of mandelic acid oxidation. Comparisons of adsorption and reaction among mandelic acid, methyl mandelate, and atrolactic acid suggest that Cr^{VI} adsorption is required for the reaction to take place, while the adsorption of organic reductant may be unnecessary. The reaction, to our surprise, is zero order with respect to mandelic acid, but fractional order with respect to the ester methyl mandelate. This change in reaction order indicates that Cr^{VI} reduction by mandelic acid and methyl mandelate occurs via different rate-limiting steps.

Introduction

Aquatic environments contain a variety of dissolved and particulate constituents that determine pathways and rates of pollutant chemical reactions. In addition to serving as stoichiometric reagents, dissolved and particulate constituents can catalyze or inhibit hydrolysis, autoxidation, photolysis, and a number of other important reactions (1, 2).

Hydrous oxides, carbonates, clays, and other minerals with surface areas of hundreds of meters²/gram are widespread in soils, sediments, and aquifers (3). Catalysis of hydrolysis reactions and oxidation-reduction reactions by hydrous oxides has been firmly established. Al_2O_3 catalyzes the hydrolysis of monophenyl terephthalate by accumulating ester and nucleophile (OH^-) at the oxide/water interface, thereby increasing their encounter frequency (4). FeOOH and TiO_2 catalyze the hydrolysis of phenyl picolinate by forming surface chelates with the carbonyl oxygen and pyridyl nitrogen of the ester, thereby increasing the electrophilicity of the carbonyl carbon and

increasing rates of nucleophilic attack (5). Adsorption of VO^{II} , Mn^{II} , and Fe^{II} onto hydrous oxide surfaces increases rates of autoxidation in some instances by several orders of magnitude (6-9). Adsorption is believed to change the electronic structure of the metal ion in ways that facilitate complex formation and subsequent electron transfer with molecular oxygen (10).

Chromium is a priority metal pollutant (11) and potential carcinogen (12-14) that exists in two major oxidation states in aquatic environments. Cr^{VI} occurs as the highly soluble oxyanions HCrO_4^- and CrO_4^{2-} ; "anion-like" Cr^{VI} adsorption onto hydrous oxide surfaces increases as the pH decreases (15-17). Cr^{III} exists as $\text{Cr}^{3+}(\text{aq})$ and Cr^{III} hydroxo complexes in solution, and as low-solubility phases such as $\text{Cr}(\text{OH})_3(\text{s})$ and $(\text{Cr},\text{Fe})(\text{OH})_3(\text{s})$ (16, 18); "cation-like" Cr^{III} adsorption increases as the pH is increased (19). For these reasons, changes in oxidation state have a dramatic effect on chromium solid/solution partitioning and subsurface migration rates.

The oxidation of Cr^{III} by molecular oxygen and by MnO_2 is thermodynamically favorable near neutral pH (20, 21). Direct reaction with molecular oxygen is exceedingly slow, as evidenced by the long residence times of Cr^{III} within oxygenated surface waters (22-24). The observation that Cr^{III} is oxidized more rapidly in high-Mn-content soils than other types implies that higher-valent manganese is involved in the oxidation process (21). Well-controlled laboratory studies on pyrolusite ($\beta\text{-MnO}_2$) oxidation of Cr^{III} confirm this observation and further demonstrate that Cr^{III} must first adsorb before oxidation by surface-bound Mn^{IV} can take place (25).

Cr^{VI} reduction by many inorganic and organic reductants occurs in acid solution. The kinetics and mechanism of Cr^{VI} reduction by Fe^{II} and other inorganic reductants has been reviewed by Espenson (26). Cr^{VI} reduction by many classes of organic compounds such as alkanes, alcohols, aldehydes, ketones, and aliphatic and aromatic acids as well as nitrogen- and sulfur-containing compounds has been reviewed by Westheimer (27), Stewart (28), and Cainelli and Cardillo (29).

The challenge is to extrapolate information from the chemistry literature toward higher, more environmentally relevant pH conditions. Studies of Cr^{VI} reduction by Fe^{II} have been extended to near neutral pH (30, 31); the reaction reaches completion within 1 or 2 min after the addition of Fe^{II} ions (31). Fe^{II} is believed to contribute at least partly to Cr^{VI} reduction in subsurface soils (32), mildly reducing sand and gravel aquifers (33), and anoxic lakes (34). Cr^{VI} reduction near neutral pH also occurs rapidly in the presence of reduced sulfur compounds such as $\text{H}_2\text{S}/\text{HS}^-$ (30, 35) and thiols (36, 37). Many subsurface environments contain only negligible amounts of Fe^{II} , $\text{H}_2\text{S}/\text{HS}^-$, and organic thiols. In these situations, a large fraction of the reductant capacity is composed of compounds possessing alcoholic, carbonyl, and carboxylic acid functional groups. Direct Cr^{VI} reduction by compounds possessing these functional groups is typically slow near neutral pH, however (36, 38), with half-lives of years in some cases (39).

Dissolved and particulate constituents occurring in natural environments may alter reaction rates between Cr^{VI} and natural organic compounds. The objective of the

* E-mail address: dog_zats@jhvmhs.hcf.jhu.edu.

[†] Present address: AL/EQC, 139 Barnes Drive, Suite 2, Tyndall AFB, FL 32403-5323; e-mail address: baolin_deng@ccmail.aeq.tyndall.af.mil.

present work is to investigate whether hydrous oxide surfaces can catalyze Cr^{VI} reduction. TiO₂ was selected for study because of its strong Lewis acid properties, as demonstrated in earlier studies of surface-catalyzed reactions (5). Mandelic acid was selected because it possesses the same reductant moiety found in important α -hydroxyl carboxylic acids such as glycolic acid (HCH(OH)CO₂H), lactic acid (CH₃CH(OH)CO₂H), malic acid (HO₂CCH₂CH(OH)CO₂H), and tartaric acid (HO₂CCH(OH)CH(OH)CO₂H), and because the parent compound and oxidation products can be readily monitored by HPLC. Reactions with methyl mandelate and atrolactic acid are also examined in order to get insights into the reaction mechanisms.

Materials and Methods

Reagents. All solutions and suspensions were prepared using 18 M Ω ·cm resistivity distilled deionized water (DDW, Millipore Corp.). Glassware was cleaned using 5 N HNO₃ and thoroughly rinsed with DDW prior to use. Stock potassium dichromate and other inorganic salt solutions were prepared from analytical-grade reagents (J. T. Baker) and filtered through 0.2 μ m membrane filters (Nuclepore Corp.) prior to use. Organic reagents from Fisher Scientific (diphenylcarbazide, ACS reagent grade), Sigma Chemical Co. (benzaldehyde), and Aldrich Chemical Co. (mandelic acid, atrolactic acid hemihydrate, methyl mandelate, sodium benzoylformate, methyl benzoylformate, and benzoic acid) were used without further purification. Organic stock solutions were prepared daily.

Titanium dioxide (TiO₂, type 25, primarily anatase) was obtained from Degussa Corp. and used as received. A specific surface area of 40.5 m²/g was determined for this material according to BET single-point nitrogen adsorption (40). Acid–base titration performed at different NaNO₃ electrolyte concentrations indicate a p*H*_{zpc} (pH of zero proton condition) of 6.5 (5). A 10 g/L TiO₂ stock suspension was prepared using DDW and stirred with a Teflon-coated magnetic stir bar.

Cr^{VI} Reduction Experiments. Preparation of the reaction suspension began by adding stock K₂Cr₂O₇, acetic acid, sodium acetate, NaClO₄, and organic stock solution to 50 mL amber bottles. The TiO₂ stock suspension and all bottles were sparged with argon for 30 min before being transferred to an inert atmosphere (5% H₂, N₂ balance) glovebox, which employed a palladium catalyst to remove traces of O₂ (Coy Laboratory Products, Inc.). Within the glovebox, 5 mL of 10 g/L TiO₂ stock suspension was added to each bottle using a disposable tip pipettor (Gilson Corp.). The reproducibility of TiO₂ delivery was evaluated by pipetting stock suspension into six vials, drying the suspensions at 110 °C for 12 h, and then weighing the dried material. A maximum error of 1.1% was found. Each bottle was then sealed with a silicon rubber/Teflon septum and placed in a 25 °C constant temperature bath and stirred with a Teflon-coated magnetic stir bar.

Unless otherwise stated, reaction suspensions contained 20 μ M total Cr^{VI}, 1.0 g/L TiO₂, 5.0 mM acetic acid/sodium acetate (to maintain constant pH), and 0.10 M NaClO₄ (to maintain constant ionic strength). pH was measured directly in the TiO₂ suspensions at the ends of experiments. Samples were collected at specified time intervals and were filtered using 0.2 μ m membrane filters (Nuclepore Corp.) prior to Cr^{VI} and organic analysis in supernatant solutions.

Adsorption Experiments. Suspensions containing TiO₂ and adsorbates were prepared according to the procedures

described for the Cr^{VI} reduction experiments. The extent of adsorption was calculated as the difference between total added adsorbate concentration and the supernatant concentration. This procedure is valid only when no significant chemical transformation of the adsorbate takes place. For this reason, Cr^{VI} and organic compound adsorption experiments were performed in separate suspensions. Slow decomposition of mandelic acid in the presence of O₂ required that the adsorption experiments be performed in an inert atmosphere glovebox.

Chemical Analysis. Cr^{VI} concentration in supernatant solution ([Cr^{VI}]_{aq}) was determined using the diphenylcarbazide colorimetric method (41) in which stoichiometric oxidation of the diphenylcarbazide reagent yielded a product with an absorption peak at 540 nm. Phosphoric acid instead of sulfuric acid was used to control medium acidity as suggested by Pilkington and Smith (42), and 2.5 $\times 10^{-2}$ M NaH₂PO₄/H₃PO₄ buffer (pH 2.12) was most appropriate. Organic compounds which react quickly with Cr^{VI} under the acidic conditions of the colorimetric test (43) or absorb light at 540 nm represent possible interferences to the colorimetric method. Preliminary experiments indicated that the organic reactants and products examined in this study did not interfere with the colorimetric method.

Organic reductants (mandelic acid, methyl mandelate, and atrolactic acid) and their reaction intermediates and products (benzaldehyde, benzoylformic acid, methyl benzoylformate, and benzoic acid) in supernatant solutions were analyzed by HPLC using a μ Bondapak C18 column (Waters Corp.) and UV detector. A gradient method employing methanol and 5 mM trifluoroacetic acid eluents was required for efficient organic separation. The organic analytes were identified by comparison of retention times with those of authentic standards under different chromatographic conditions.

Results and Discussion

In the heterogeneous system under investigation, four reactions in parallel contribute to overall Cr^{VI} reduction, yielding the four terms in the differential equation listed below:

$$-d[\text{Cr}^{\text{VI}}]_{\text{T}}/dt = k_1[\text{Cr}^{\text{VI}}]_{\text{aq}}[\text{MA}]_{\text{aq}} + k_2[\text{Cr}^{\text{VI}}]_{\text{aq}}[\text{MA}]_{\text{ads}} + k_3[\text{Cr}^{\text{VI}}]_{\text{ads}}[\text{MA}]_{\text{aq}} + k_4[\text{Cr}^{\text{VI}}]_{\text{ads}}[\text{MA}]_{\text{ads}} \quad (1)$$

where MA represents mandelic acid, the subscripts aq and ads refer to dissolved and adsorbed species concentrations, and the subscript T stands for total. In order to distinguish among these four contributing reactions, the extents of Cr^{VI} and mandelic acid adsorption must be evaluated under the reaction conditions employed in the reduction experiments and compared with rates of Cr^{VI} reduction. Indirect evidence regarding contributions from the four terms listed above can be obtained by examining how changes in pH and reductant concentration, changes in organic structure, and addition of nonreacting adsorbates affect overall rates of Cr^{VI} reduction.

Cr^{VI} Reduction by α -Hydroxy Carboxylic Acids in Homogeneous Solution. The reaction of 20 μ M Cr^{VI} and 200 μ M mandelic acid was examined in catalyst-free solutions between pH 3.2 and 6.7 (acetate buffer). During a time period of 150 h, no Cr^{VI} reduction was observed.

Under more strongly acidic conditions, Cr^{VI} reduction by mandelic acid and by other α -hydroxyl carboxylic acids

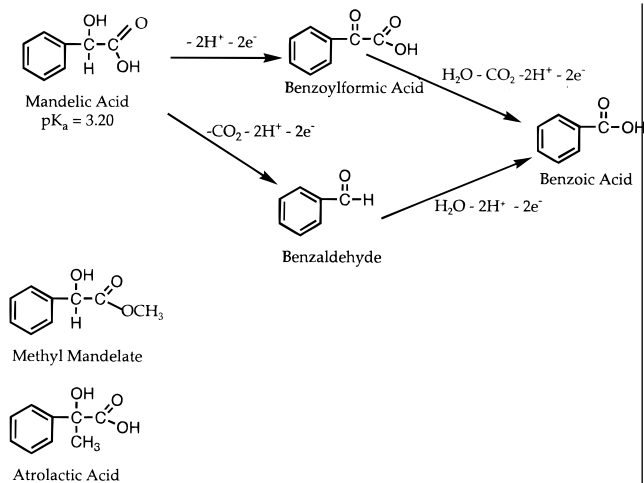


FIGURE 1. Possible pathways for the oxidation of mandelic acid by Cr^{VI} (based upon Jain et al. (45) and Ip and Rocek (47, 48)). The structures of methyl mandelate and atrolactic acid, used to probe the mechanism of the surface-catalyzed reaction, are shown for comparison.

is considerably more rapid and has been studied in considerable detail (44–48). Although the acidity (pH < 3.0) used in these studies is beyond the range of most natural systems, the studies do provide information regarding reaction products, stoichiometry, and mechanism.

Identification of organic oxidation products plays an important role in deducing reaction mechanism. Oxidation of α -hydroxyl carboxylic acids by Cr^{VI} begins with formation of a chromate–organic reductant adduct, which undergoes rate-limiting electron transfer and decomposition by cleavage at the α -carbon hydrogen bond and at the α -carbon–carboxylate carbon bond (29, 49). In the case of lactic acid, one-electron oxidants (e.g., Mn^{III} and Ce^{IV}) yield principally acetaldehyde and CO₂, the products of carbon–carbon fission, while two-electron oxidants (e.g., V^V, Ti^{III}) produce pyruvic acid, the product of carbon–hydrogen fission (45).

Three-electron reduction of Cr^{VI} to Cr^{III} generally requires two or more elementary reactions in series, generating Cr^V and Cr^{IV} intermediate oxidation states (50). It is therefore possible for Cr^{VI} oxidation of α -hydroxyl carboxylic acids to proceed by both carbon–hydrogen and carbon–carbon fission, yielding both α -carbonyl carboxylic acids and aldehydes (44–46). Indeed, α -hydroxyl carboxylic acids yield products in markedly different ratios of α -carbonyl carboxylic acids and aldehydes, indicating differing differences in the prevailing reaction mechanism (46, 48, 51).

Figure 1 indicates possible pathways for Cr^{VI} oxidation of mandelic acid, the principal reductant considered in this work. Benzoylformic acid, the product of carbon–hydrogen bond fission, and benzaldehyde, the product of carbon–carbon bond fission, can both be further oxidized to benzoic acid. The structures of methyl mandelate and atrolactic acid, which will be used to probe reaction mechanism, are also shown in Figure 1.

Organic Compound Adsorption. The extent of mandelic acid adsorption onto 1.0 g/L TiO₂ was monitored as a function of time at pH 3.3, 4.7, and 6.3. In each case, adsorption reached a maximum value within 2 h. In all subsequent experiments, mandelic acid and other organic analytes were added to TiO₂ suspensions 24 h prior to the adsorption measurement.

As the pH is decreased from 6.0 to 3.2 (Figure 2), mandelic acid adsorption onto TiO₂ gradually increases. This result

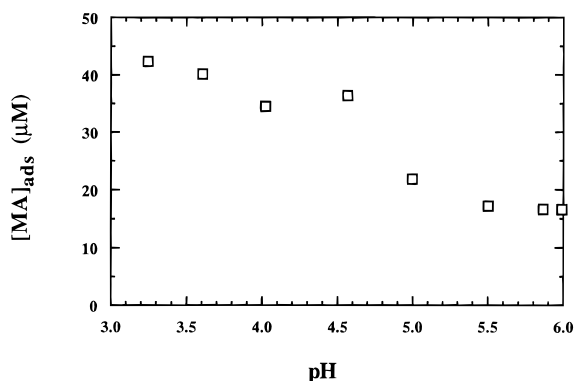


FIGURE 2. pH isotherm for the adsorption of 200 μ M mandelic acid onto 1.0 g/L TiO₂.

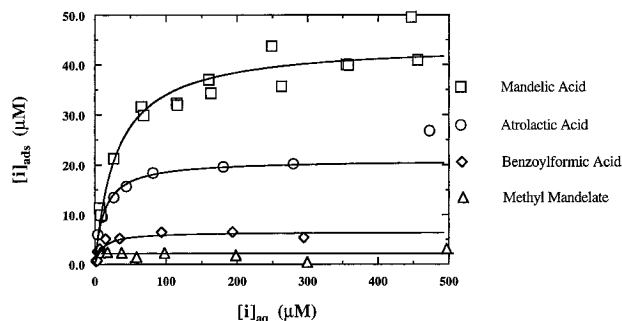


FIGURE 3. Concentration isotherms for adsorption of mandelic acid, atrolactic acid, benzoylformic acid, and methyl mandelate onto 1.0 g/L TiO₂ at pH 4.7 (all reaction suspensions contain 5.0 mM acetate buffer and 0.10 M NaClO₄).

is in agreement with earlier studies of carboxylic acid adsorption onto amorphous Fe(OH)₃ (15), Al₂O₃ (52), and α -FeOOH (goethite) (53). In all cases, adsorption increases with decreasing pH until a maximum value is attained at a pH equal to the pK_a of the carboxylic acid group.

The adsorption of mandelic acid, atrolactic acid, benzoylformic acid, and methyl mandelate onto 1.0 g/L TiO₂ at fixed pH (4.7) as a function of concentration is shown in Figure 3. The amount of adsorbed organic analyte ([i]_{ads}) is expressed in terms of micromole of adsorption in 1 L of suspension (μ M), and the total dissolved concentration ([i]_{aq}) is in terms of micromole of analyte in 1 L of supernatant (μ M). For each compound, adsorption increases as the concentration is increased until a limiting value is reached. The initial slope of the [i]_{ads} versus [i]_{aq} plot and the limiting value of [i]_{ads} both decrease in the following order: mandelic acid > atrolactic acid > benzoylformic acid \gg methyl mandelate. The adsorption maximum, obtained by fitting adsorption data to the Langmuir adsorption model, is 44.2 μ M for mandelic acid, 20.9 μ M for atrolactic acid, and 6.5 μ M for benzoylformic acid. Methyl mandelate possesses an aliphatic alcohol and a carbonyl ligand donor group. The negligible adsorption of this compound indicates that these two ligand-donor groups alone have a poor ability to form surface complexes in comparison to compounds possessing free carboxylate groups. Among compounds possessing free carboxylate groups, those with an α -hydroxyl group adsorb more strongly than those with an α -carbonyl group.

Cr^{VI} Adsorption. Cr^{VI} adsorption onto 1.0 g/L TiO₂ was examined as a function of time at three pH values (3.3, 4.7, and 6.3) to establish adsorption rates. More than 85% of Cr^{VI} adsorption was obtained within 5 min, and maximum

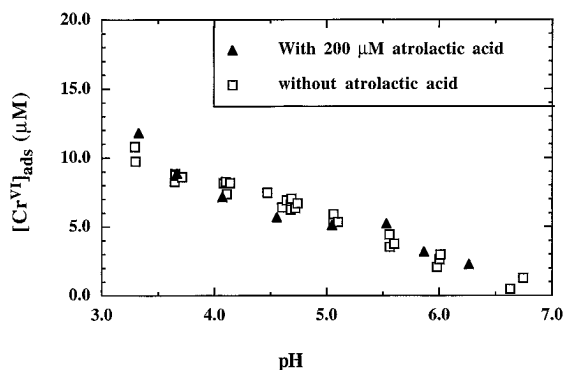


FIGURE 4. pH isotherm for the adsorption of 20 μM Cr^{VI} onto 1.0 g/L TiO_2 in the presence and absence of 200 μM atrolactic acid.

values were obtained within 1 h. In all subsequent experiments, Cr^{VI} was added to TiO_2 suspensions 12 h prior to the adsorption measurement.

The adsorption of 20 μM Cr^{VI} onto 1.0 g/L TiO_2 is shown as a function of pH in Figure 4. Cr^{VI} adsorption increases in nearly a linear fashion as the pH is decreased from 6.8 to 3.2. A similar pH dependence was observed for Cr^{VI} adsorption onto kaolinite under comparable Cr^{VI} concentration conditions (54). Cr^{VI} adsorption on aluminum oxide (55) and goethite (17), however, shows stronger pH dependence.

Cr^{VI} adsorption onto 1.0 g/L TiO_2 at pH 4.7 increases as a function of increasing Cr^{VI} concentrations, as shown in Figure 5A. Applying the Langmuir adsorption model to this data yields a value of S_T (maximum Cr^{VI} adsorption) equal to 39 μM and a value of K_s (the adsorption constant) equal to 0.012 μM^{-1} .

$$S + \text{Cr}^{\text{VI}}_{\text{aq}} = \text{Cr}^{\text{VI}}_{\text{ads}} \quad K_s = \frac{[\text{Cr}^{\text{VI}}]_{\text{ads}}}{[S][\text{Cr}^{\text{VI}}]_{\text{aq}}} \quad (2)$$

This equation can be combined with the mass balance equation for surface sites ($[S] + [\text{Cr}^{\text{VI}}]_{\text{ads}} = S_T$), resulting in the following expression for $[\text{Cr}^{\text{VI}}]_{\text{ads}}$:

$$[\text{Cr}^{\text{VI}}]_{\text{ads}} = \frac{K_s S_T [\text{Cr}^{\text{VI}}]_{\text{aq}}}{1 + K_s [\text{Cr}^{\text{VI}}]_{\text{aq}}} \quad (3)$$

As the smooth curve in the figure indicates, this model provides a reasonable fit to the experimental adsorption data. Most Cr^{VI} reduction experiments discussed in later sections employed total Cr^{VI} concentrations of 20 μM , yielding $[\text{Cr}^{\text{VI}}]_{\text{aq}}$ less than 15 μM . At such low Cr^{VI} concentrations, the Langmuir adsorption isotherm (eq 3) can be simplified to a linear adsorption isotherm (eq 4). As shown in Figure 5B, close agreement with the linear adsorption isotherm is observed when $[\text{Cr}^{\text{VI}}]_{\text{aq}}$ is in this concentration range.

$$[\text{Cr}^{\text{VI}}]_{\text{ads}} = K_s S_T [\text{Cr}^{\text{VI}}]_{\text{aq}} \quad (4)$$

The presence of both Cr^{VI} and organic substrate may cause competitive adsorption to take place. Surface-catalyzed Cr^{VI} reduction by mandelic acid is sufficiently fast that it interferes with the determination of Cr^{VI} adsorption. Atrolactic acid does not reduce Cr^{VI} in the presence of TiO_2 (discussed in later sections), but adsorbs in a fashion similar to that of mandelic acid. Atrolactic acid can therefore be used to examine the nature and extent of competitive adsorption.

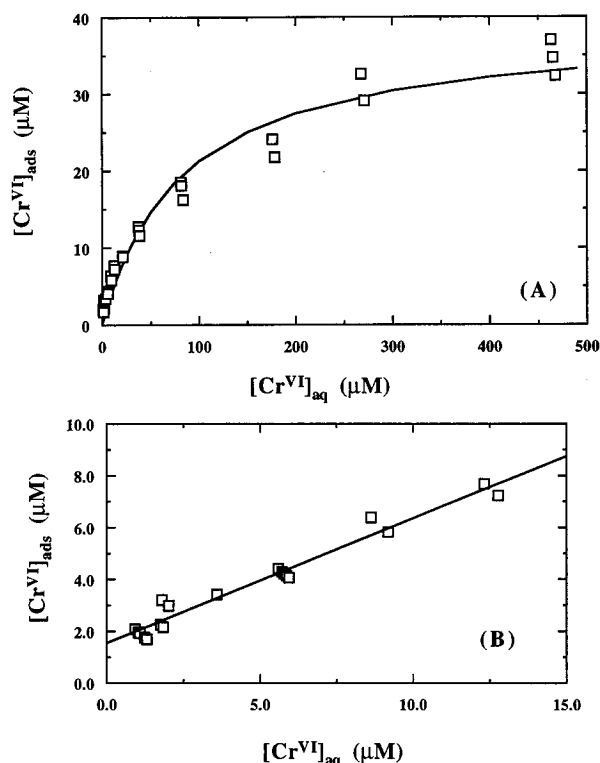


FIGURE 5. Concentration isotherm for Cr^{VI} adsorption onto 1.0 g/L TiO_2 at pH 4.7: (A) entire concentration isotherm; (B) close-up of the linear range at low $[\text{Cr}^{\text{VI}}]_{\text{aq}}$.

As Figure 4 indicates, 200 μM atrolactic acid has a negligible effect on the adsorption of 20 μM Cr^{VI} onto 1.0 g/L TiO_2 , throughout the pH range considered. In a separate experiment performed at pH 4.7, the atrolactic concentration was increased to 500 μM ; a slight decrease in Cr^{VI} adsorption (less than 12%) was observed.

We can infer, on the basis of the observation that atrolactic acid does not interfere with Cr^{VI} adsorption under the conditions of the Cr^{VI} reduction experiments, that competitive adsorption between Cr^{VI} and mandelic acid does not take place. This conclusion may no longer be valid when a different organic reductant or different hydrous oxide is employed. Mesuere and Fish (56), for example, observed that oxalic acid interferes with Cr^{VI} adsorption onto goethite.

TiO_2 -Catalyzed Cr^{VI} Reduction. In order to investigate whether or not surface catalysis takes place, solutions initially containing 20 μM $[\text{Cr}^{\text{VI}}]_{\text{aq}}$ (total dissolved Cr^{VI}) were monitored as a function of time in the presence and absence of mandelic acid and TiO_2 . Figure 6 reports the results of these experiments performed using 5 mM acetate buffer (pH 4.7) and 0.10 M NaClO_4 . Curve A indicates that negligible reaction takes place between Cr^{VI} and 200 μM mandelic acid in the absence of TiO_2 during nearly 60 h of reaction. Curve B, representing experiments in which both 200 μM mandelic acid and 1.0 g/L TiO_2 are present, consists of two stages. The rapid initial decrease in $[\text{Cr}^{\text{VI}}]_{\text{aq}}$ by approximately 7 μM is caused by Cr^{VI} adsorption onto TiO_2 , as discussed earlier (Figures 4 and 5). The gradual decrease in $[\text{Cr}^{\text{VI}}]_{\text{aq}}$ that continues for the duration of the experiments requires that both mandelic acid and TiO_2 be present in the system; removing TiO_2 by filtration (curve C) prevents further decrease in $[\text{Cr}^{\text{VI}}]_{\text{aq}}$.

Curves A–C serve as proof of the existence of TiO_2 -catalyzed reaction between Cr^{VI} and mandelic acid. The

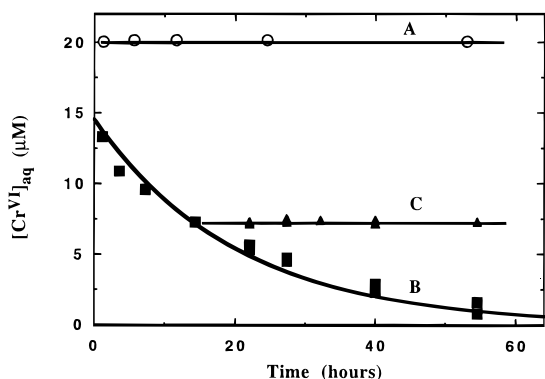


FIGURE 6. Reduction of 20 μM Cr^{VI} by 200 μM mandelic acid at pH 4.7 as a function of time in (A) TiO_2 -free solution and in (B) 1.0 g/L TiO_2 suspension. (C), TiO_2 removal by filtration following 14 h of reaction eliminates the surface catalytic effect.

loss of catalytic activity upon filtration indicates that it is the TiO_2 surface that serves as the catalyst, rather than dissolved species released by the TiO_2 surface.

Reaction Products and Reaction Stoichiometry. As discussed earlier, 200 μM atrolactic acid (and, by analogy, mandelic acid) does not interfere with Cr^{VI} adsorption. In addition, $[\text{Cr}^{\text{VI}}]_{\text{T}}$ (total dissolved plus adsorbed Cr^{VI} or $[\text{Cr}^{\text{VI}}]_{\text{aq}} + [\text{Cr}^{\text{VI}}]_{\text{ads}}$) concentrations below 20 μM are within the linear range of the concentration adsorption isotherm (Figure 5). Thus, $[\text{Cr}^{\text{VI}}]_{\text{ads}}$ and $[\text{Cr}^{\text{VI}}]_{\text{T}}$ as a function of time can be estimated in reaction suspensions using $[\text{Cr}^{\text{VI}}]_{\text{aq}}$ measured in supernatant solution and a proportionality constant for adsorption.

Peaks for mandelic acid, benzoylformic acid, benzaldehyde, and benzoic acid in supernatant solutions recovered by filtration exhibited the same HPLC retention times as authentic standards. (HPLC eluent compositions were changed to confirm that shifts in retention times matched those of the authentic standards.) An attempt was made to recover oxidation products from TiO_2 particles collected by centrifugation using $1.0 \times 10^{-2} \text{ M NaOH}$. Benzoylformic acid was detectable in these samples, while benzaldehyde and benzoic acid were not.

Adsorbed benzoylformic acid concentrations can be estimated using measurements of supernatant solution concentrations and the adsorption isotherm presented in Figure 3. Benzaldehyde does not adsorb to any significant extent.

Figure 7 shows dissolved plus adsorbed concentrations of Cr^{VI} , mandelic acid, benzoylformic acid, and benzaldehyde as a function of time at pH 4.7. $[\text{Cr}^{\text{VI}}]_{\text{T}}$ decreases exponentially and is accompanied by the production of benzoylformic acid and benzaldehyde. At any point in the reaction, the benzoylformic acid concentration is at least 3 times higher than the benzaldehyde concentration, making it the principal oxidation product under the conditions employed here. Figure 7 also shows the increase in dissolved benzoic acid concentration as the reaction progresses. Even when the adsorption of benzoic acid is accounted for (comparable to the other carboxylic acids), benzoic acid represents only a minor product during the first 80 h of the reaction.

Benzoylformic acid and benzaldehyde are both two-electron-oxidation products of mandelic acid, and therefore the stoichiometric equivalents of Cr^{VI} consumed are the same:

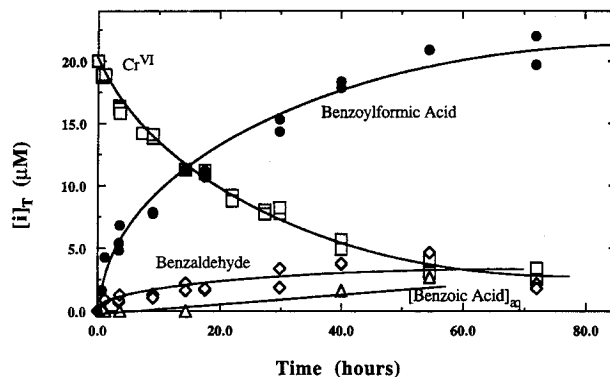
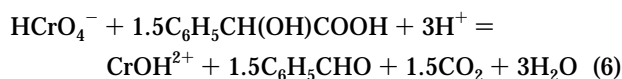
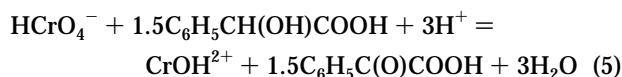
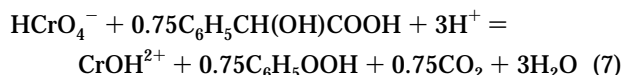


FIGURE 7. Net decrease of 20 μM Cr^{VI} and production of benzoylformic acid, benzaldehyde, and benzoic acid in suspensions containing 200 μM mandelic acid and 1.0 g/L TiO_2 at pH 4.7. $[i]_{\text{T}}$ (dissolved plus adsorbed concentration) was calculated from supernatant concentrations and the concentration adsorption isotherms presented in Figures 3 and 5.



Additional two-electron oxidation of benzoylformic acid and benzaldehyde yields benzoic acid, thereby altering the stoichiometry of Cr^{VI} reduction:



The 10-fold excess of mandelic acid in the experiment reported in Figure 7 makes it difficult to measure the concentration decrease of mandelic acid caused by reaction with Cr^{VI} . The sum of benzoylformic acid concentration and benzaldehyde concentration does, however, approximate the concentration of mandelic acid consumed. Dividing this sum by the consumed amount of Cr^{VI} yields a ratio quite close to 1.5, which remains constant as the reaction progresses. The close agreement between this experimentally-determined ratio and ratios predicted by reactions 5 and 6 serves to confirm this reaction stoichiometry.

Comparison among Mandelic Acid, Methyl Mandelate, and Atrolactic Acid. Modifications to the mandelic acid structure can provide information regarding reaction mechanism. In the case of methyl mandelate (structure shown in Figure 1), the carboxylate group has been blocked, causing adsorption to drop to nearly negligible levels (Figure 3). In the case of atrolactic acid, the hydrogen atom at the α -carbon has been replaced by a methyl group, causing a slight decrease in the extent of adsorption.

The reactivity of the three reductants was compared in experiments employing 20 μM Cr^{VI} , 200 μM reductant, and a pH 4.7 buffer. In the absence of TiO_2 , none of the reductants reduced significant amounts of Cr^{VI} . In the presence of TiO_2 , an initial, rapid loss in $[\text{Cr}^{\text{VI}}]_{\text{aq}}$ arising from adsorption is always observed (Figure 8). The continued loss of $[\text{Cr}^{\text{VI}}]_{\text{aq}}$ indicative of surface-catalyzed reduction is, however, only observed with mandelic acid and methyl mandelate. During 160 h of reaction, no TiO_2 -catalyzed Cr^{VI} reduction by atrolactic acid takes place.

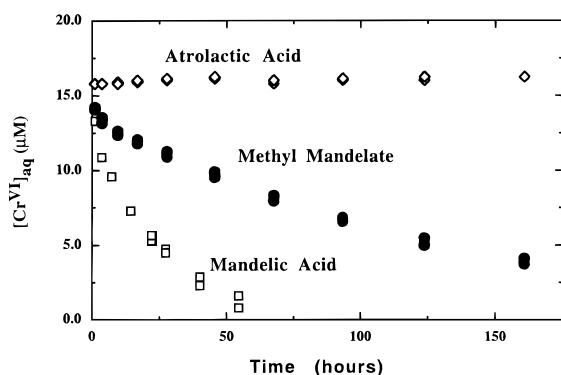


FIGURE 8. Reduction of 20 μM Cr^{VI} by 200 μM mandelic acid, methyl mandelate, and atrolactic acid (pH 4.7, 1.0 g/L TiO_2).

As discussed earlier, removing TiO_2 by filtration causes Cr^{VI} reduction to cease, indicating that one or more of the reactants must adsorb in order for catalysis to occur. For the three structurally similar reductants, the ability to adsorb onto TiO_2 (mandelic acid > atrolactic acid \gg methyl mandelate) is not correlated with the rate at which Cr^{VI} is reduced (mandelic acid > methyl mandelate \gg atrolactic acid). It can therefore be concluded that catalysis arises from the adsorption of Cr^{VI} , corresponding to either the third or the fourth term in eq 1. Adsorption of reductant may be a contributing factor but may be unnecessary.

Mandelic acid reduces Cr^{VI} in TiO_2 suspensions more quickly than methyl mandelate. In strongly acidic, homogeneous solutions, glycolic acid ($\text{H}_2\text{C}(\text{OH})\text{COOH}$) reduces Cr^{VI} more quickly than ethyl glycolate ($\text{H}_2\text{C}(\text{OH})\text{COOCH}_2\text{CH}_3$) (46). The diminished reactivity of methyl and ethyl esters both in the presence and in the absence of catalytic surfaces indicates that electronic (or steric) effects are responsible, rather than differences in adsorption properties.

Cr^{VI} reduction by atrolactic acid in TiO_2 suspensions is negligible. In strongly acidic, homogeneous solutions, Cr^{VI} reduction by atrolactic acid occurs at one-tenth the rate observed with mandelic acid (46). Loss of the CH_3 substituent (as $^+\text{CH}_3$ or CH_3^+) required to form either the α -carbonyl carboxylic acid or the aldehyde oxidation products shown in Figure 1 apparently limits the reaction with atrolactic acid.

Effect of pH. The effect of pH on TiO_2 -catalyzed reduction is shown in Figure 9A. This set of experiments employed 1.0 g/L TiO_2 , 20 μM Cr^{VI} , and 200 μM mandelic acid. The pH was changed by varying the relative concentration of acetic acid and sodium acetate comprising the 5.0 mM acetate buffer. Under these conditions, the mandelic acid concentration is nearly constant as the reaction progresses. Plots of $\log[\text{Cr}^{\text{VI}}]_{\text{aq}}$ as a function of time are linear, indicating that the reaction is first order with respect to $[\text{Cr}^{\text{VI}}]_{\text{aq}}$.

$$-d[\text{Cr}^{\text{VI}}]_{\text{aq}}/dt = k_{\text{obs}}[\text{Cr}^{\text{VI}}]_{\text{aq}} \quad (8)$$

Slopes of $\log[\text{Cr}^{\text{VI}}]_{\text{aq}}$ versus time plots yield the pseudo-first-order rate constant k_{obs} , in units of h^{-1} .

Cr^{VI} adsorption is fast relative to the time scales of the reduction reaction. According to the linear relationship of low Cr^{VI} adsorption (eq 4), total Cr^{VI} can be expressed as

$$[\text{Cr}^{\text{VI}}]_{\text{T}} = [\text{Cr}^{\text{VI}}]_{\text{aq}} + [\text{Cr}^{\text{VI}}]_{\text{ads}} = (1 + K_{\text{s}}S_{\text{T}})[\text{Cr}^{\text{VI}}]_{\text{aq}} \quad (9)$$

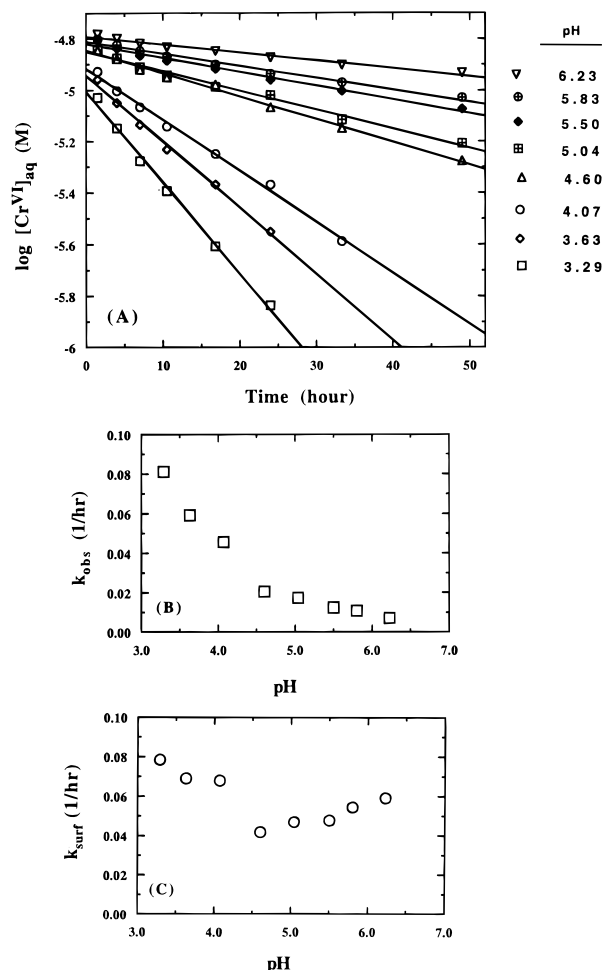


FIGURE 9. Effect of pH on TiO_2 -catalyzed Cr^{VI} reduction by mandelic acid: (A) linear plots of $\log [\text{Cr}^{\text{VI}}]_{\text{aq}}$ as a function of time indicating first-order reaction; (B) observed pseudo-first-order rate constant k_{obs} as a function of pH; (C) pseudo-first-order rate constant in terms of adsorbed Cr^{VI} (k_{surf}) as a function of pH. (Reaction conditions: 20 μM Cr^{VI} , 200 μM mandelic acid, 1.0 g/L TiO_2 .)

Since Cr^{VI} reduction in homogeneous solution is insignificant, the first two terms in eq 1 can be ignored, yielding

$$-d[\text{Cr}^{\text{VI}}]_{\text{T}}/dt = (1 + K_{\text{s}}S_{\text{T}})(d[\text{Cr}^{\text{VI}}]_{\text{aq}}/dt) = (k_3[\text{Red}]_{\text{aq}} + k_4[\text{Red}]_{\text{ads}})[\text{Cr}^{\text{VI}}]_{\text{ads}} \quad (10)$$

$$-d[\text{Cr}^{\text{VI}}]_{\text{aq}}/dt = \frac{(k_3[\text{Red}]_{\text{aq}} + k_4[\text{Red}]_{\text{ads}})[\text{Cr}^{\text{VI}}]_{\text{ads}}}{1 + K_{\text{s}}S_{\text{T}}} \quad (11)$$

$$-d[\text{Cr}^{\text{VI}}]_{\text{aq}}/dt = k_{\text{surf}}[\text{Cr}^{\text{VI}}]_{\text{ads}} \quad (12)$$

According to this definition, k_{surf} is the pseudo-first-order rate constant for the reduction of adsorbed Cr^{VI} . Comparison of eqs 11 and 12 indicates that k_{surf} may change as the reductant concentration is increased and the ratio of $[\text{Red}]_{\text{aq}}$ to $[\text{Red}]_{\text{ads}}$ is changed. Since both K_{s} and the ratio of $[\text{Red}]_{\text{aq}}$ to $[\text{Red}]_{\text{ads}}$ are functions of pH, k_{surf} may also change as a function of pH. As long as Cr^{VI} concentrations are within the linear range of the adsorption isotherm, k_{surf} is not a function of $[\text{Cr}^{\text{VI}}]_{\text{T}}$. Comparison of eqs 8 and 12 indicates that

$$k_{\text{surf}} = k_{\text{obs}}[\text{Cr}^{\text{VI}}]_{\text{aq}}/[\text{Cr}^{\text{VI}}]_{\text{ads}} \quad (13)$$

As the pH is decreased from 6.23 to 3.29, $[\text{Cr}^{\text{VI}}]_{\text{ads}}$ increases

TABLE 1

Pseudo-First-Order Rate Constants (k_{obs}) for Cr^{VI} Reduction by Mandelic Acid in the Presence of 1.0 g/L TiO_2 (pH 4.7 Buffered by 5 mM Acetate, 0.10 M NaClO_4)

test	$[\text{Cr}^{\text{VI}}]_{\text{T}}$ (μM)	[mandelic acid] _T (μM)	$[\text{TiO}_2]$ (g/L)	k_{obs} (1/h)	r^2	data points
A1	20	30	1.0	5.17×10^{-2}	0.9764	3
A2	20	40	1.0	5.08×10^{-2}	0.9964	4
A3	20	50	1.0	5.37×10^{-2}	0.9888	4
A4	20	60	1.0	5.36×10^{-2}	0.9837	4
A5	20	80	1.0	4.35×10^{-2}	0.9900	5
A6	20	100	1.0	3.88×10^{-2}	0.9833	6
A7	20	150	1.0	3.97×10^{-2}	0.9890	6
A8	20	200	1.0	4.07×10^{-2}	0.9888	6
A9	20	300	1.0	4.25×10^{-2}	0.9905	6
A10	20	400	1.0	4.32×10^{-2}	0.9879	6
A11	20	500	1.0	4.17×10^{-2}	0.9909	6
B1	20	100	1.0	3.22×10^{-2}	0.9979	6
B2	20	200	1.0	3.71×10^{-2}	0.9958	6
B3	20	300	1.0	3.75×10^{-2}	0.9964	6
B4	20	400	1.0	3.75×10^{-2}	0.9980	6
C1	60	60	1.0	1.68×10^{-2}	0.9750	3
C2	60	80	1.0	1.74×10^{-2}	0.9986	4
C3	60	100	1.0	2.21×10^{-2}	0.9950	4
C4	60	150	1.0	1.71×10^{-2}	0.9898	5
C5	60	200	1.0	1.83×10^{-2}	0.9900	6
C6	60	300	1.0	1.76×10^{-2}	0.9970	7
C7	60	400	1.0	1.86×10^{-2}	0.9964	7
C8	60	500	1.0	1.97×10^{-2}	0.9964	7
D1	120	40	1.0	1.19×10^{-2}	0.9995	3
D2	120	50	1.0	1.31×10^{-2}	0.9938	3
D3	120	70	1.0	1.37×10^{-2}	0.9979	3
D4	120	100	1.0	1.48×10^{-2}	0.9980	4

by a factor of 4.77 (calculated from the data shown in Figure 4). As pH is decreased within the same range, k_{obs} increases by a factor of 11.5 (Figure 9B). However, k_{surf} only changes by a factor of 1.9 within this pH range (Figure 9C). It can therefore be concluded that changes in the extent of Cr^{VI} adsorption are largely responsible for changes in the rate of surface-catalyzed reduction as a function of pH. Interpreting the small changes in k_{surf} as a function of pH should be done with caution, since the extent of Cr^{VI} adsorption and the rate of the surface-catalyzed reaction diminish substantially as the pH is increased above 5.0.

Effect of Reactant Concentration. By examining how reaction rates change as a function of Cr^{VI} and organic reductant concentration, it is possible to determine reaction orders with respect to each reactant. Experiments of this kind also identify situations where the reaction is limited by the supply of catalytic surfaces or reactant.

Experiments examining Cr^{VI} reduction by mandelic acid and by methyl mandelate performed at fixed pH (5 mM acetate, pH 4.7) and oxide loading (1.0 g/L TiO_2) are reported in Tables 1 and 2, respectively. As already mentioned, Cr^{VI} reduction by both mandelic acid and methyl mandelate in the absence of TiO_2 is negligible at this pH; the surface reaction dominates. In order for pseudo-first-order conditions to apply, the reductant concentration must be kept constant. For this reason, data points in which more than 20% of added reductant had been consumed were rejected from calculation of k_{obs} values. In the tables, all experiments begun on the same day are designated by the same letter. Day-to-day comparisons (A6/B1, A8/B2, A9/B3, A10/B4) yield rate constants (k_{obs}) that vary from 6 to 17%.

TABLE 2

Pseudo-First-Order Rate Constants (k_{obs}) for Cr^{VI} Reduction by Methyl Mandelate in the Presence of 1.0 g/L TiO_2 (pH 4.7 Buffered by 5 mM acetate, 0.10 M NaClO_4)

test	$[\text{Cr}^{\text{VI}}]_{\text{T}}$ (μM)	[methyl mandelate] _T (μM)	$[\text{TiO}_2]$ (g/L)	k_{obs} (1/h)	r^2	data points
P1	20	40	1.0	5.38×10^{-3}	0.9012	5
P2	20	60	1.0	6.40×10^{-3}	0.9762	7
P3	20	80	1.0	7.55×10^{-3}	0.9782	7
P4	20	100	1.0	6.71×10^{-3}	0.9866	8
P5	20	200	1.0	1.11×10^{-2}	0.9944	8
P6	20	400	1.0	1.79×10^{-2}	0.9977	7
P7	20	760	1.0	2.47×10^{-2}	0.9983	7
Q1	120	40	1.0	2.30×10^{-4}	0.9469	7
Q2	120	50	1.0	3.90×10^{-4}	0.9846	6
Q3	120	70	1.0	4.47×10^{-4}	0.9704	6
Q4	120	100	1.0	6.54×10^{-4}	0.9896	7

TABLE 3

Effect of Increasing Total Cr^{VI} Concentration on k_{obs} for TiO_2 -Catalyzed Reaction with Mandelic Acid and Methyl Mandelate (pH 4.7, 5 mM Acetate Buffer, 100 μM Reductant, 1.0 g/L TiO_2 , 0.10 M NaClO_4)

total Cr^{VI} (μM)	fraction of Cr^{VI} adsorbed (%)	k_{obs} (mandelic acid) (1/h)	k_{obs} (methyl mandelate) (1/h)
20	30	3.55×10^{-2} (A6, B1)	6.71×10^{-3} (P4)
60	23	2.21×10^{-2} (C3)	
120	17	1.48×10^{-2} (D4)	6.54×10^{-4} (Q4)

For mandelic acid, the change in k_{obs} with increasing reductant concentration is small, within the same range as the day-to-day differences just discussed (Table 1). Empirically, k_{obs} is related to the reductant concentration in the following manner:

$$k_{\text{obs}} = k'_{\text{obs}}[\text{Red}]^n \quad (14)$$

A plot of $\log k_{\text{obs}}$ versus $\log [\text{Red}]$ yields the reaction order n . According to this approach, the reaction is zeroth-order with respect to the mandelic acid concentration.

In the case of the methyl mandelate ester, the increase in k_{obs} with increasing methyl mandelate concentration is quite substantial. Equation 14 was applied to the results from experiments presented in Table 2. Using the 20 μM Cr^{VI} data (seven points, with r^2 equal to 0.974), the $\log k_{\text{obs}}$ plot yields a fractional reaction order with respect to methyl mandelate of 0.53. Using the 120 μM Cr^{VI} data (four points, with r^2 equal to 0.915), the $\log k_{\text{obs}}$ plot yields a reaction order of 1.0.

By whatever comparison is applied, methyl mandelate reduces Cr^{VI} more slowly than mandelic acid. In experiments employing 20 μM Cr^{VI} , k_{obs} values for methyl mandelate are only 10–40% of k_{obs} values for mandelic acid. In experiments employing 120 μM Cr^{VI} , k_{obs} values for methyl mandelate are only 2–4.5% of values for mandelic acid.

Results from Tables 1 and 2 pertaining to the effect of Cr^{VI} concentration on k_{obs} are summarized in Table 3. The pH (4.7) and reductant concentration are the same in all

experiments. When Cr^{VI} concentrations are increased to 60 and 120 μM , adsorption lies outside the linear range of the isotherm shown in Figure 5. As a consequence, the fraction of total Cr^{VI} in the adsorbed state decreases from 30% at 20 μM Cr^{VI} to 17% at 120 μM Cr^{VI} . k_{obs} decreased by an even greater amount: 58% for reaction with mandelic acid and 90% for reaction with methyl mandelate. Thus, the reduction rate per mole of adsorbed Cr^{VI} decreases as $[\text{Cr}^{\text{VI}}]_{\text{ads}}$ is increased.

Effect of Phosphate. Because Cr^{VI} must adsorb in order for TiO_2 -catalyzed reduction to take place, other solutes which compete with Cr^{VI} for available surface sites may inhibit the reaction. Phosphate merits examination, because of its widespread occurrence in aquatic environments and its strong adsorption onto soil minerals (57) and onto TiO_2 in particular (58).

A preliminary experiment examined the effect of increasing phosphate concentrations on the adsorption of 20 μM Cr^{VI} and 200 μM mandelic acid in two separate 1.0 g/L TiO_2 suspensions (pH 4.7). Increasing the phosphate concentration from 0.0 to 500 μM caused an 11-fold decrease in Cr^{VI} adsorption, from 6.1 to 0.57 μM , slightly above our analytical detection limit of 0.44 μM . Increasing the phosphate concentration from 0.0 to 500 μM caused a 4-fold decrease in mandelic acid adsorption, from 35.6 to 8.8 μM .

TiO_2 -catalyzed reduction of Cr^{VI} (20 μM) by mandelic acid (200 μM) or methyl mandelate (200 μM) was examined in the presence and absence of 500 μM phosphate. In the absence of phosphate, an initial rapid drop in $[\text{Cr}^{\text{VI}}]_{\text{aq}}$ is observed. In the presence of phosphate, this initial rapid drop disappears. Initial rates were calculated by linear regression employing all data points up to the point where 30% of Cr^{VI} had been reduced. The reaction rate with mandelic acid decreased by a factor of 4.7 in the presence of 500 μM phosphate, while the reaction rate with methyl mandelate decreased by a factor of 8.3.

The rate decrease in the presence of phosphate is believed to be caused by phosphate adsorption, which diminishes surface sites available for reactant adsorption. It is unclear, however, whether diminished Cr^{VI} adsorption or diminished reductant adsorption is primarily responsible for decreased reaction rates. As has been previously discussed, the surface-catalyzed reaction is believed to require Cr^{VI} adsorption and must therefore take place via the last two terms in eq 1. If adsorption of Cr^{VI} alone is necessary, reaction via the third term dominates, and a nearly 11-fold decrease in k_{obs} would be expected for either reductant. If adsorption of both Cr^{VI} and mandelic acid is necessary, reaction via the fourth term dominates, and a 44-fold decrease in k_{obs} would be expected. The 4.7-fold decrease actually observed with mandelic acid is most consistent with reaction dominated by the third term in eq 1. The fact that inhibition is less than expected may be an indication that the surface is heterogeneous; phosphate may have a slight preference for noncatalytic sites. (Reaction with methyl mandelate cannot be evaluated in this way, since changes in the low levels of methyl mandelate adsorption are not discernible.)

Reaction Mechanism. Any proposed mechanism for TiO_2 -catalyzed Cr^{VI} reduction by mandelic acid must accommodate the following observations:

(i) Cr^{VI} adsorption on the surface is required for the reaction to occur. Within the linear range of the Cr^{VI} adsorption isotherm, the reaction is first order with respect

to $[\text{Cr}^{\text{VI}}]_{\text{ads}}$. As the Cr^{VI} concentration is increased beyond the linear range, the reaction rate per mole of adsorbed Cr^{VI} decreases with increasing $[\text{Cr}^{\text{VI}}]_{\text{ads}}$.

(ii) Adsorption of the organic reductant may be unnecessary for the surface-catalyzed reaction to occur, although mandelic acid does adsorb to a significant extent. Mandelic acid adsorption does not significantly alter $[\text{Cr}^{\text{VI}}]_{\text{ads}}$.

(iii) Rates of Cr^{VI} and organic reductant adsorption are much faster than overall rates of surface-catalyzed redox reaction (a few minutes versus several hours or days).

(iv) Mandelic acid yields the fastest surface-catalyzed reaction. A zeroth-order dependence on mandelic acid concentration is observed. Methyl mandelate, which reacts more slowly, yields a first-order dependence at low methyl mandelate concentrations and a fractional-order dependence at high methyl mandelate concentrations.

(v) Surface-catalyzed Cr^{VI} reduction by mandelic acid obeys the reaction stoichiometry represented by eqs 5 and 6. Benzoylformic acid is the principal oxidation product; benzaldehyde is the secondary product.

Observation iv provides an important clue regarding the reaction mechanism. The transition of first-order to fractional-order reductant concentration dependence observed with methyl mandelate and the zeroth-order dependence observed with mandelic acid indicate that one or both of the other reactants (Cr^{VI} or catalytic surface sites) have become saturated with reductant. Wilkins (59) presented an empirical expression for reactions of this kind that exhibit such "saturation kinetics". For the present reaction, this expression can be written as

$$-\frac{d[\text{Cr}^{\text{VI}}]_{\text{T}}}{dt} = \frac{a[\text{Cr}^{\text{VI}}]_{\text{ads}}[\text{Red}]_{\text{aq}}}{1 + b[\text{Red}]_{\text{aq}}} \quad (15)$$

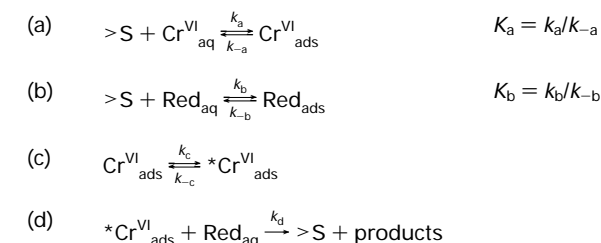
In the case of mandelic acid, $b[\text{Red}]_{\text{aq}} \gg 1.0$ throughout the range of mandelic acid concentration considered, resulting in zeroth-order dependence. In the case of methyl mandelate, values of both a and b are changed. At low methyl mandelate concentrations, $b[\text{Red}]_{\text{aq}} \ll 1$ and the reaction is first order with respect to reductant. At high methyl mandelate concentrations, $b[\text{Red}]_{\text{aq}}$ increases in magnitude, yielding the observed fractional dependence.

According to Wilkins (59), saturation kinetics can arise in three ways: (1) reactants react in a "dead-end" or nonproductive equilibrium that competes with the forward reaction; (2) reactants rapidly form a precursor complex prior to a slower, rate-limiting step; or (3) one of the reactants becomes activated prior to reaction. In the present case, mechanisms 1 and 2 would involve the formation of a Cr^{VI} -reductant complex in solution or a Cr^{VI} -reductant- TiO_2 ternary complex on the surface, which should change the ratio of dissolved to adsorbed Cr^{VI} . Since increasing reductant concentrations had only a negligible effect on Cr^{VI} adsorption, these mechanisms are unlikely.

Mechanism 3, illustrated in Table 4, provides the best explanation for the experimental observations. Cr^{VI} and reductant adsorption (reactions a and b) are treated as pre-equilibrium reactions because they are fast relative to subsequent steps. Noting the strong dependence of the overall reaction rate on adsorbed Cr^{VI} (in marked contrast to the negligible dependence on adsorbed reductant), we postulate that formation of the activated species $^*\text{Cr}^{\text{VI}}_{\text{ads}}$

TABLE 4

Proposed Reaction Mechanism



(reaction c) must occur before electron transfer and product formation (reaction d).

According to this scheme, the following two rate equations can be written:

$$\frac{d[P]}{dt} = k_d[Red]_{aq}[*Cr^{VI}]_{ads} \quad (16)$$

$$\frac{d[*Cr^{VI}]_{ads}}{dt} = k_c[Cr^{VI}]_{ads} - (k_{-c} + k_d[Red]_{aq})[*Cr^{VI}]_{ads} \quad (17)$$

The steady-state approximation can be applied to eq 17, yielding an expression for $[*Cr^{VI}]_{ads}$, which can be inserted into eq 16:

$$\frac{d[P]}{dt} = \frac{(k_c k_d / k_{-c})[Red]_{aq}[Cr^{VI}]_{ads}}{1 + (k_d / k_{-c})[Red]_{aq}} \quad (18)$$

In agreement with experiment, the overall reaction rate is proportional to $[Cr^{VI}]_{ads}$. Comparison with eq 15 reveals that $a = k_c k_d / k_{-c}$ and $b = k_d / k_{-c}$. In the case of mandelic acid, k_d is sufficiently high that $(k_d / k_{-c})[Red]_{aq}$ is much greater than 1.0 throughout the range of reductant concentrations examined, and overall reaction is limited by reaction c, the activation of adsorbed Cr^{VI} . Replacing mandelic acid by methyl mandelate lowers the value of k_d , causing a shift in the rate-limiting step to Reaction d, especially at low reductant concentrations.

Reaction c, the activation of adsorbed Cr^{VI} , serves to explain why time scales of overall reaction (approximately 18 h at pH 4.7) are so much longer than time scales of Cr^{VI} adsorption (a few minutes). Activation may arise from the transition from outer- to inner-sphere adsorption, the diffusion from inactive to active surface sites, the exchange of ligands at the Cr^{VI} center, or other phenomena that alter the stoichiometry, structure, and reactivity of adsorbed Cr^{VI} .

Although the initial reduction of Cr^{VI} appears to be rate-limiting, subsequent reactions involving Cr^V and Cr^{IV} will play a major role in overall reaction stoichiometry. Ample evidence exists that three higher-valent forms of chromium exhibit different selectivity toward available reductants and often yield different organic reaction products (38, 46, 49). Hasan and Rocek (46), for example, observed oxidation of glycolic acid to glyoxylic acid, formaldehyde, and carbon dioxide in a 2:1:1 ratio, and they related this ratio to the relative production of Cr^V and Cr^{IV} . In our work, mandelic acid bears the same reactive functional group as glycolic acid and yields a similar ratio of the acid (benzoylformic acid) to the aldehyde (benzaldehyde). Thus, a detailed

examination of the role of Cr^V and Cr^{IV} in the overall reaction may be fruitful.

Concluding Remarks

This work demonstrates that TiO_2 surfaces dramatically catalyze the reduction of Cr^{VI} by mandelic acid and highlights the importance of adsorbed Cr^{VI} in the reaction mechanism. To fully evaluate the effect of surfaces on Cr^{VI} reduction in soils, sediments, and other aquatic environments, additional work must evaluate whether other naturally-occurring mineral surfaces (e.g., oxides, aluminosilicates, carbonates) and other naturally-occurring reductants also participate in surface-catalyzed Cr^{VI} reduction. These points will be addressed in the second paper in this series.

Acknowledgments

The support by the Environmental Engineering Program of the U.S. National Science Foundation (Grant No. BCS8918091) under the direction of Dr. Edward H. Bryan is gratefully acknowledged. Prof. Werner Stumm (EAWAG, Switzerland) and William Fish (Oregon Graduate Institute of Science and Technology) provided numerous useful comments during the completion of this work.

Literature Cited

- Hoffmann, M. *Environ. Sci. Technol.* **1980**, *14*, 1061–1066.
- Hoffmann, M. In *Aquatic Chemical Kinetics*; Stumm, W., Ed.; Wiley & Sons: New York, 1990; pp 71–111.
- Hillel, D. *Fundamentals of Soil Physics*; Academic Press: New York, 1980; pp 65–68.
- Stone, A. T. *J. Colloid Interface Sci.* **1989**, *127*, 429–441.
- Torrents, A.; Stone, A. T. *Environ. Sci. Technol.* **1991**, *25*, 143–149.
- Diem, D.; Stumm, W. *Geochim. Cosmochim. Acta* **1984**, *48*, 1571–1573.
- Sung, W.; Morgan, J. J. *Geochim. Cosmochim. Acta* **1981**, *45*, 2377–2383.
- Wehrli, B.; Stumm, W. *Langmuir* **1988**, *4*, 753–758.
- Davies, S. H. R.; Morgan, J. J. *J. Colloid Interface Sci.* **1989**, *129*, 63–77.
- Wehrli, B.; Sulzberger, B.; Stumm, W. *Chem. Geol.* **1989**, *78*, 167–179.
- U.S. Environmental Protection Agency. *Fed. Regist.* **1987**, *52* (74), 12866–12874.
- Venitt, S.; Levy, L. S. *Nature* **1974**, *250*, 493–495.
- Borges, K. M.; Wetterhahn, K. E. *Carcinogenesis* **1989**, *10*, 2165–2168.
- Nieboer, E.; Shaw, S. L. In *Chromium in the Natural and Human Environment*; Nriagu, J. O., Nieboer, E., Eds.; Wiley & Sons: New York, 1988.
- Davis, J. A.; Leckie, J. O. *J. Colloid Interface Sci.* **1980**, *74*, 32–43.
- Rai, D.; Zachara, J. M.; Eary, L. E.; Girvin, D. C.; Moore, D. A.; Resch, C. T.; Sass, B. M.; Schmidt, R. L. *Geochemical Behavior of Chromium Species*. Report EPRI-4544; Battelle, Pacific Northwest Laboratories: Richland, WA, 1986.
- Mesuer, K.; Fish, W. *Environ. Sci. Technol.* **1992**, *26*, 2357–2364.
- Ray, D.; Sass, B. M.; Moore, D. A. *Inorg. Chem.* **1987**, *26*, 345–349.
- Griffin, R. A.; Au, H. K.; Frost, R. R. *J. Environ. Sci. Health, Part A* **1977**, *12*, 431–449.
- Elderfield, H. *Earth Planet. Sci. Lett.* **1970**, *9*, 10–16.
- Bartlett, R. J.; James, B. J. *J. Environ. Qual.* **1979**, *8*, 31–35.
- Cranston, R. E.; Murray, J. W. *Anal. Chim. Acta* **1978**, *99*, 275–282.
- Murray, J. W.; Spell, B.; Paul, B. In *Trace Metals in Sea Water*; Wong, C. S., Boyle, E., Bruland, K., Burton, J. D., Goldberg, E. D., Eds.; Plenum: New York, 1983; pp 643–640.
- Ahern, F.; Eckert, J. M.; Payne, N. C.; Williams, K. L. *Anal. Chim. Acta* **1985**, *175*, 147–151.
- Eary, L. E.; Rai, D. *Environ. Sci. Technol.* **1987**, *21*, 1187–1193.
- Espenson, J. H. *J. Acc. Chem. Res.* **1970**, *3*, 347–353.
- Westheimer, F. H. *Chem. Rev.* **1949**, *45*, 419–451.
- Stewart, R. *Oxidation Mechanisms: Application to Organic Chemistry*; W. A. Benjamin, Inc.: New York, 1964.

- (29) Cainelli, G.; Cardillo, G. *Chromium Oxidations in Organic Chemistry*; Springer-Verlag: New York, 1984.
- (30) Schroeder, D. C.; Lee, G. F. *Water, Air, Soil Pollut.* **1975**, *4*, 155–365.
- (31) Eary, L. E.; Rai, D. *Environ. Sci. Technol.* **1988**, *22*, 972–977.
- (32) Eary, L. E.; Rai, D. *Soil Sci. Soc. Am. J.* **1991**, *55*, 676–683.
- (33) Anderson, L. D.; Kent, D. B.; Davis, J. A. *Environ. Sci. Technol.* **1994**, *28*, 178–185.
- (34) Johnson, C. A.; Sigg, L.; Lindauer, U. *Limnol. Oceanogr.* **1992**, *37* (2), 315–321.
- (35) Smillie, R. H.; Hunter, K.; Loutit, M. *Water Res.* **1981**, *15*, 1351–1354.
- (36) Connett, P. H.; Wetterhahn, K. E. *J. Am. Chem. Soc.* **1985**, *107*, 4282–4288.
- (37) Kwong, D. Ph.D. Dissertation, Baylor University, Waco, TX, 1990.
- (38) Krumpolc, M.; Rocek, J. *Inorg. Chem.* **1985**, *24*, 617–621.
- (39) Elovitz, M. S.; Fish, W. *Environ. Sci. Technol.* **1994**, *28*, 2161–2169.
- (40) Brunauer, S.; Emmett, P. H.; Teller, E. *J. Am. Chem. Soc.* **1938**, *60*, 309.
- (41) APHA, AWWA, WPCF. *Standard Methods for the Examination of Water and Wastewater*, 17th ed.; American Public Health Association: Washington, 1989; pp 201–204.
- (42) Pilkington, E. S.; Smith, P. R. *Anal. Chim. Acta* **1967**, *39*, 321–328.
- (43) Harzdorf, A. C. *Int. J. Environ. Anal. Chem.* **1987**, *29*, 249–261.
- (44) Kemp, T. J.; Waters, W. A. *J. Chem. Soc. (London)* **1964**, 1192–1194.
- (45) Jain, C. L.; Shanker, R.; Bakore, G. V. *Indian J. Chem.* **1969**, *7*, 159–160.
- (46) Hasan, F.; Rocek, J. *J. Am. Chem. Soc.* **1975**, *97*, 1444–1450.
- (47) Ip, D.; Rocek, J. *J. Org. Chem.* **1979**, *44*, 312–313.
- (48) Ip, D.; Rocek, J. *J. Am. Chem. Soc.* **1979**, *101*, 6311–6319.
- (49) Beattie, J. K.; Haight, G. P. *Prog. Inorg. Chem.* **1972**, *17*, 93–145.
- (50) Cannon, R. D. *Electron Transfer Reactions*; Butterworths: London, 1980.
- (51) Haight, G. P.; Jursich, G. M.; Kelso, M. T.; Merrill, P. J. *Inorg. Chem.* **1985**, *24*, 2740–2746.
- (52) Kummert, R.; Stumm, W. *J. Colloid Interface Sci.* **1980**, *75*, 373–385.
- (53) Balistrieri, L. S.; Murray, J. W. *Geochim. Cosmochim. Acta* **1987**, *51*, 1151–1160.
- (54) Zachara, J. M.; Cowan, C. E.; Schmidt, R. L.; Ainsworth, C. C. *Clays Clay Miner.* **1988**, *36*, 317–326.
- (55) Honeyman, B. D. Ph.D. Dissertation, Stanford University, Menlo Park, CA, 1984.
- (56) Mesuere, K.; Fish, W. *Environ. Sci. Technol.* **1992**, *26*, 2365–2370.
- (57) James, B. R.; Bartlett, R. J. *J. Environ. Qual.* **1983**, *12*, 177–181.
- (58) Torrents, A.; Stone, A. T. *Environ. Sci. Technol.* **1993**, *27*, 1060–1067.
- (59) Wilkins, R. G. *Kinetics and Mechanism of reaction of transition metals*, 2nd ed.; VCH: New York, 1991.

Received for review March 7, 1995. Revised manuscript received September 5, 1995. Accepted September 6, 1995.[®]

ES950156C

[®] Abstract published in *Advance ACS Abstracts*, December 1, 1995.